Xiaoli He[1], Xi Yang[2], Peng Guo[3], Taohai Ran[4]

[1] Second Clinical College, Chongqing Medical University, Chongqing, China

[2] Shapingba Hospital affiliated with Chongqing University, Department of Ultrasound Medicine,Chongqing, China

[3] General Electric Medical Systems Trading Development (Shanghai) Co., LTD, Shanghai, China

[4] Second Affiliated Hospital of Chongqing Medical University, Department of Ultrasound Medicine, Chongqing, China

Evaluation of Left Atrial Function in Patients with Hypertensive Heart Disease and Preserved Ejection Fraction Using Real-Time, Three-Dimensional Speckle Tracking Imaging

Objective — This research investigated the application of real-time, three-dimensional speckle tracking imaging (RT-3D-STI) to evaluate left atrial (LA) function in individuals suffering from hypertensive heart disease (HHD) and heart failure with preserved ejection fraction (HFpEF).

Material and methods — This retrospective study included 100 patients with HHD and HFpEF hospitalized from August 2023 to June 2024 (HFpEF group). 100 healthy individuals undergoing physical examinations comprised the control group. Patient data were collected, and echocardiography was performed to measure LA diameter (LAD), left ventricular end diastolic diameter (LVEDD), interventricular septal thickness (IVST), left ventricular posterior wall thickness (LVPWT), left ventricular outflow tract diameter (LVOTd), early diastolic maximum velocity of mitral valve inflow (MVE), late diastolic maximum velocity of mitral valve inflow (MVA), early diastolic and late diastolic velocities of mitral annulus measured by tissue Doppler ultrasound (e' and a'), tricuspid annular plane systolic excursion (TAPSE), and left ventricular ejection fraction (LVEF). The LA images were analyzed using GE software, and the following parameters were measured: L emptying fraction (LAEF), LA emptying volume (LAEV), LA volume at the onset of contraction (LAVpreA), minimum LA volume (LAVmin), maximum LA volume (LAVmax), LA strain during the reservoir phase (LASr), LA strain during the contraction phase (LASct), and LA strain during the conduit phase (LAScd). ROC curves were adopted to evaluate the diagnostic value of LA parameters for HFpEF, and a Pearson correlation analysis examined the relationship between these parameters and N-terminal pro-B-type natriuretic peptide (NT-proBNP).

Results — Compared with the control group, the blood pressure in the HFpEF group was significantly higher ($p<0.05$). In the HFpEF group, NT-proBNP concentrations were significantly greater than those observed in the control group ($p<0.05$). No statistically significant variances were detected in LVEF, LVEDD, LVOTd, TAPSE, MVE, MVA, ratio of E wave velocity to A wave velocity (E/A), a', LAEV, LAVmin, or LAVpreA between the two groups ($p>0.05$). Compared to the control group, the HFpEF group had dramatically higher LAD, IVST, and LVPWT ($p<0.05$). The HFpEF group also had lower e', LAEF, LASr, LAScd, and LASct, while E/e', maximum LA volume index (LAV Imax), and LAVmax were higher ($p<0.05$). LASr was negatively associated with NT-proBNP ($r=-0.255$, $p=0.016$), whereas no significant correlation was found among LAScd, LASct, and NT-proBNP ($P>0.05$).

Conclusion — LA strain parameters can serve as a non-invasive method for quantitatively assessing LA dysfunction in patients with HFpEF.

Keywords — Real-time three-dimensional speckle tracking imaging; hypertensive heart disease; preserved ejection fraction; heart failure; left atrial function

For citations — Xiaoli He, Xi Yang, Peng Guo, Taohai Ran. Evaluation of Left Atrial Function in Patients with Hypertensive Heart Disease and Preserved Ejection Fraction Using Real-Time, Three-Dimensional Speckle Tracking Imaging. Kardiologiia. 2025;65(8):63–70. [Russian: Сяоли Хэ, Си Ян, Пэн Го, Таохай Ран. Оценка функции левого предсердия у пациентов с гипертонической болезнью и сохраненной фракцией выброса левого желудочка с использованием трехмерной визуализации Speckle tracking в реальном времени. Кардиология. 2025;65(8):63–70].

Corresponding author — Taohai Ran. E-mail: ranhaitao@hospital.cqmu.edu.cn

Introduction

Hypertension has become one of the most widespread chronic conditions across the globe, impacting more than 25% of the world's population. It can cause serious damage to the cardiovascular and cerebrovascular systems and stands as a major contributor to the global disease burden [1]. Prolonged elevation of systemic blood pressure beyond normal levels leads to pathophysiological changes in myocardial

Central illustration. Evaluation of Left Atrial Function in Patients with Hypertensive Heart Disease and Preserved Ejection Fraction Using Real-Time, Three-Dimensional Speckle Tracking Imaging

Patient selection

HFpEF group (n=100, heart failure with preserved ejection fraction)

Data collection

LA images (GE software)

Control group (n=100, healthy individuas)

Data collection

LA images (GE software)

Statistical analysis

ROC-curve

Correlation analysis

Conventional echocardiography parameters

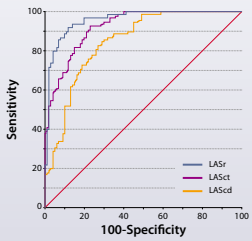

Table 6. Correlation analysis between LA strain parameters and NT-proBNP in HFpEF patients

Variables	NT-proBNP	
	r	p
LASr	–0.255	0.016
LAScd	–0.168	0.132
LASct	–0.203	0.079

LASr, LA strain during the reservoir phase; LAScd, LA strain during the conduit phase; LASct, LA strain during the contraction phase.

Table 2. Comparison of conventional echocardiography parameters between the two groups

Variable	HFpEF group (n=100)	Control group (n=100)	t	p
LAD (mm)	34.65±5.22	28.71±3.48	9.468	<0.001
LVEF (%)	58.85±6.43	59.12±5.24	0.326	0.745
LVEDD (mm)	46.33±3.79	45.97±4.01	0.652	0.515
IVST (mm)	9.76±0.91	8.23±0.85	12.287	<0.001
LVPWT (mm)	9.89±1.22	9.05±1.36	4.600	<0.001
LVOTd (mm)	18.55±1.86	18.49±2.77	0.180	0.858
TAPSE (mm)	18.52±2.23	17.98±1.99	1.807	0.072

Data are mean±SD. LAD, left ventricular end diastolic diameter; LVEF, left ventricular ejection fraction; LVEDD, left ventricular end diastolic diameter; IVST, interventricular septal thickness; LVPWT, left ventricular posterior wall thickness; LVOTd, left ventricular outflow tract diameter; TAPSE, tricuspid annular plane systolic excursion.

cells, resulting in geometric alterations of the heart chambers and structural changes in myocardial tissues, eventually triggering hypertensive heart disease (HHD) [2, 3]. Considering the projected increase in the hypertension burden and its impact on life expectancy over the next decade, HHD is likely to play an even more significant role in the pathophysiology of cardiovascular diseases [4].

The main clinical characteristics of hypertensive heart disease (HHD) involve left ventricular hypertrophy and dilation. If these conditions are not effectively addressed, they can readily advance to left ventricular failure or even total heart failure, potentially resulting in death [5]. Clinical evidence shows that heart failure with preserved ejection fraction (HFpEF) is among the most prevalent forms of heart failure, with HHD being a significant contributing factor in its onset [6].

More than half of the patients with unexplained exertional dyspnea are ultimately diagnosed with HFpEF after invasive examinations, and this condition shows high rates of incidence, mortality, and rehospitalization. The five-year survival rate is comparable to that of cancer, with a poor prognosis and substantial healthcare burden. Recent studies indicate that HFpEF is linked to multiple factors, such as advancing age, hypertension, coronary heart disease, atrial fibrillation, diabetes, obesity, chronic kidney disease, anemia, and feminine sex [7–9]. These factors, linked to aging, lifestyle, and genetic predisposition, promote a systemic inflammatory state, leading to structural and functional abnormalities in the heart and eventually causing HFpEF [10].

Echocardiography is a non-invasive, convenient, accurate, and repeatable method that has tremendous value in assessing cardiac structure and function. It remains the most effective tool for diagnosing heart failure and evaluating treatment outcomes [11]. Nonetheless, traditional echocardiography is characterized by subjectivity, limited views, and angle dependency, with measurements highly influenced by the operator's expertise. To address these limitations, real-time three-dimensional speckle tracking imaging (RT-3D-STI) echocardiography, an advanced imaging software technique for quantifying myocardial strain, has gained clinical attention. This technology assesses myocardial deformation in longitudinal, radial, and circumferential directions, reflecting myocardial contractile state and myocardial diastolic function, blood supply, and viability [12, 13].

ISSN 0022-9040. Кардиология. 2025;65(8). DOI: 10.18087/cardio.2025.8.n2856

Since the early changes in left atrial (LA) function in HHD patients are often subtle and since traditional echocardiography is better suited for evaluating left ventricular morphology, this study utilized RT-3D-STI to confirm whether there are accompanying abnormalities in LA myocardial function. The goal was to evaluate changes in LA function in HHD patients with HFpEF and to further explore the clinical significance of these changes.

Material and methods

Subject selection

This retrospective study incorporated 100 patients diagnosed with HHD and HFpEF who were hospitalized in the cardiovascular medicine department of our hospital between August 2023 and June 2024. These patients formed the HFpEF group. From healthy subjects who underwent physical examinations during the same timeframe, another group of 100, who were age- and risk factor-matched with the HFpEF group, was selected as the control group. The research was carried out in compliance with the Declaration of Helsinki.

Inclusion and exclusion criteria

Inclusion criteria:

1) Patients with a confirmed diagnosis of hypertension defined as systolic blood pressure (SBP) ≥140 mmHg and/or diastolic blood pressure (DBP) ≥90 mmHg.
2) Laboratory markers of cardiac function, with N-terminal pro-B-type brain natriuretic peptide (NT-proBNP) >100 pg/ml.
3) Echocardiographic measurements showing impaired left ventricular diastolic function and a left ventricular ejection fraction (LVEF) ≥50%.

Exclusion criteria: Patients with acute heart failure, serious valvular heart disease (VHD), arrhythmias, severe systemic illnesses, LVEF <50%, or with echocardiographic images of poor quality.

Data collection

General patient and subject data

The gender, age, body mass index (BMI). resting heart rate, SBP, and DBP were recorded. Each measurement was taken three times averaged. The serum T-proBNP was recorded.

Ultrasound image acquisition

Prior to the ultrasound examination, blood pressure, heart rate, and body surface area (BSA) were recorded for all subjects. The participants were placed in the left lateral decubitus position, requested to breath calmly, and connected to a synchronized electrocardiogram instrument. The imaging was performed utilizing an echocardiography device (Vivid E90; GE Healthcare) fitted with a X5–1 probe and operating at a frequency range of 3.5 to 5 MHz. Patients were instructed to hold their breath at the end of exhalation to acquire a clear full – volume image of the left ventricular endocardium. Subsequently, they were guided to click to enter the "Multi Beat" mode and continuously collect three – dimensional dynamic images spanning four cardiac cycles. Two-dimensional, M-mode, pulse and continuous wave Doppler ultrasound images, as well as tissue Doppler Imaging (TDI), were obtained from standard parasternal and apical views. Using a high frame frequency (60–80 frames/sec), enlarged images of the left atrium (LA) were captured from the four-chamber, three-chamber, and two-chamber views, with three consecutive cardiac cycles saved. Measurements were conducted following the guidelines and techniques suggested by the American Society of Echocardiography and encompassed the following: LA diameter (LAD), left ventricular end diastolic diameter (LVEDD), interventricular septal thickness (IVST), left ventricular posterior wall thickness (LVPWT), left ventricular outflow tract diameter (LVOTd), early diastolic maximum velocity of mitral valve inflow (MVE), late diastolic maximum velocity of mitral valve inflow (MVA), TDI-derived early diastolic and late diastolic velocities of mitral annulus (e' and a', respectively), tricuspid annular plane systolic excursion (TAPSE), and LVEF, which was measured using the biplane Simpson method. Each measurement was repeated three times, and the mean value was recorded.

Ultrasound image analysis and processing

After the images were saved, they were analyzed as follows by GE's cardiac ultrasound image analysis software.

1) LA image analysis of volumes: The minimum LA volume indexed to BSA (LAVmin/BSA), maximum LA volume indexed to BSA (LAVmax/BSA), and LA volume at the onset of contraction indexed to BSA (LAVpreA/BSA) were calculated by dividing LAVmin, LAVmax, and LAVpreA by BSA respectively. The LA emptying volume (LAEV) was obtained by subtracting LAVmin from LAVmax. The LA emptying fraction (LAEF) was calculated by dividing LAEV by LAVmax.
2) The following LA strain parameters were analyzed.
   A) Reservoir phase: During left ventricular systole, the LA receives blood from the pulmonary veins, accounting for approximately 40% of LA stroke volume. The LA strain during the reservoir phase (LASr) was calculated by subtracting the strain value at the end-diastole (ED) from the strain value at the end-systole (ES). This phase includes the periods of isovolumic contraction, ejection, and isovolumic relaxation of the left ventricle (LV).
   B) Conduit phase: In healthy individuals, the LA passively transfers blood to the LV during early diastole, contributing about 35% of the atrial stroke volume. The LA strain during the conduit phase (LAScd) was

Table 1. Comparison of general data between the two groups

Variable	HFpEF group (n=100)	Control group (n=100)	t	p
Gender (male/female)	65/35	71/29	0.827	0.363
Age (yrs)	50.6±5.9	51.3±6.8	0.781	0.436
BMI (kg/m²)	21.45±3.82	22.07±3.61	1.180	0.240
Heart rate (bpm)	71.2±8.8	73.0±7.3	1.559	0.121
SBP (mmHg)	143.6±15.0	127.0±13.8	8.152	<0.001
DBP (mmHg)	87.8±6.9	69.1±7.2	18.769	<0.001
NT-proBNP (pg/ml)	1983±20	71.6±12.0	810.061	<0.001

Data are ratio or mean±SD. BMI, body mass index; SBP, systolic blood pressure; DBP, diastolic blood pressure, NT-proBNP, N-terminal pro-B-type brain natriuretic peptide.

calculated by subtracting the strain value at ES from the strain value at LAVpreA.

c) Contraction phase: The LA strain during the contraction phase (LASct) was measured in all patients. It was obtained by subtracting the strain value at LAVpreA from the strain value at ED.

Statistical analysis

All data were processed and analyzed with SPSS 22.0 software. Measurement data that met the criteria for normal distribution and homogeneity of variance were expressed as mean ±standard deviation (SD), and the t-test was used for comparisons of the groups. Enumeration data are represented as percentages and analyzed using the χ^2 test. Pearson correlation analysis was conducted for evaluation of correlations, and receiver operating characteristic (ROC) curves were generated to assess the diagnostic performance of LA strain parameters for HFpEF. A p value <0.05 was considered statistically significant.

Results

General patient and subject data (Table 1)

The HFpEF group consisted of 65 males and 35 females, with an average age of 50.6±5.9 yrs. The average BMI was 21.45±3.82 kg/m², the average heart rate was 71.2±8.8 bpm, the average SBP was 143.6±15.0 mmHg, and the average DBP was 87.8±6.9 mmHg. In the control group, there were 71 males and 29 females, with an average age of 51.3±6.9 yrs. The average BMI was 22.07±3.61 kg/m², the average heart rate was 73.0±7.3 bpm, the average SBP was 127.0±13.8 mmHg, and the average DBP was 69.1±7.2 mmHg. These baseline characteristics did not differ significantly between the groups

Table 2. Comparison of conventional echocardiography parameters between the two groups

Variable	HFpEF group (n=100)	Control group (n=100)	t	p
LAD (mm)	34.65±5.22	28.71±3.48	9.468	<0.001
LVEF (%)	58.85±6.43	59.12±5.24	0.326	0.745
LVEDD (mm)	46.33±3.79	45.97±4.01	0.652	0.515
IVST (mm)	9.76±0.91	8.23±0.85	12.287	<0.001
LVPWT (mm)	9.89±1.22	9.05±1.36	4.600	<0.001
LVOTd (mm)	18.55±1.86	18.49±2.77	0.180	0.858
TAPSE (mm)	18.52±2.23	17.98±1.99	1.807	0.072

Data are mean±SD. LAD, left ventricular end diastolic diameter; LVEF, left ventricular ejection fraction; LVEDD, left ventricular end diastolic diameter; IVST, interventricular septal thickness; LVPWT, left ventricular posterior wall thickness; LVOTd, left ventricular outflow tract diameter; TAPSE, tricuspid annular plane systolic excursion.

Table 3. Comparison of Doppler ultrasound parameters between the two groups

Variable	HFpEF group (n=100)	Control group (n=100)	t	p
MVE (m/s)	0.81±0.53	0.84±0.62	0.378	0.713
MVA (cm²)	0.93±0.21	0.92±0.13	0.405	0.686
E/A	0.83±0.15	0.80±0.12	1.562	0.120
e' (m/s)	0.06±0.01	0.11±0.03	15.811	<0.001
a'	0.09±0.04	0.10±0.04	1.768	0.079
E/e' (m/s)	12.23±1.18	8.25±0.92	26.600	<0.001
LAV Imax (ml/m²)	41.59±5.46	27.68±3.85	20.821	<0.001

Data are mean±SD. MVE, early diastolic maximum velocity of mitral valve inflow; MVA, late diastolic maximum velocity of mitral valve inflow; E/A, ratio of E wave velocity to A wave velocity; e', early diastolic mitral annular velocity; a' late diastolic mitral annular velocity; E/e', the ratio of the peak velocity of early mitral inflow (E-wave) to the peak velocity of early diastolic mitral annular motion (e' – wave); LAV Imax, maximum LA volume index.

ISSN 0022-9040. Кардиология. 2025;65(8). DOI: 10.18087/cardio.2025.8.n2856

Table 4. Comparison of LA strain parameters between the two groups

LA strain variables	HFpEF group (n=100)	Control group (n=100)	t	p
LAEF (%)	43.65±5.33	54.69±4.97	15.149	<0.001
LAEV (ml)	23.71±2.16	23.15±2.05	1.880	0.062
LAVmax (ml)	66.94±5.74	42.83±5.23	31.048	<0.001
LAVmin (ml)	20.83±2.03	20.45±1.85	1.384	0.168
LAVpreA (ml)	35.27±3.11	34.91±3.56	0.762	0.447
LASr (%)	30.61±2.88	38.45±2.97	18.951	<0.001
LAScd (%)	16.33±1.54	20.14±1.89	15.628	<0.001
LASct (%)	15.70±1.26	18.22±1.74	11.730	<0.001

Data are mean ± SD. LAEF, LA emptying fraction; LAEV, LA emptying volume; LAVmax, maximum LA volume; LAVmin, minimum LA volume; LAVpreA, LA volume at the onset of contraction; LASr, LA strain during the reservoir phase; LAScd, LA strain during the conduit phase; LASct, LA strain during the contraction phase.

Table 5. Analysis of ROC curve results for LA strain parameters

Variables	AUC	95%CI	Sensitivity (%)	Specificity (%)	Cut-off	Youden index	p
LASr	0.959	0.934~0.985	92.00	88.00	≤34.65	0.800	<0.001
LAScd	0.849	0.796~0.902	83.00	73.00	≤17.85	0.560	<0.001
LASct	0.925	0.891~0.959	93.00	77.00	≤17.02	0.700	<0.001

AUC, area under the ROC curve; CI, confidence interval.

(p>0.05). The NT-proBNP concentration in the HFpEF cohort was 1983±20 pg/ml, notably higher (p<0.05) than that of the control cohort, 71.62±11.98 pg/ml. Compared with the control group, both SBP and DBP in the HFpEF group were significantly higher (p<0.05).

Conventional echocardiography parameters (Table 2)

No statistically significant differences were detected between the two cohorts in terms of LVEF, LVEDD, LVOTd, or TAPSE (p>0.05). Compared to the control group, LAD, IVST, and LVPWT were significantly elevated in the HFpEF cohort (p<0.05). These findings demonstrate that, as opposed to healthy individuals, HFpEF patients exhibited more pronounced abnormalities in conventional echocardiographic parameters.

Doppler ultrasound parameters (Table 3)

No statistically significant differences were found between the two cohorts for MVE, MVA, E/A, and a' (p>0.05). Within the HFpEF group, the e', E/e', and LAV Imax values were (0.06±0.01) m/s, (12.23±1.18) m/s, and (41.59±5.46) ml/m^2, respectively. Compared with the control group, the e' value was lower, while the E/e' and LAV Imax values were higher within the HFpEF cohort, with these differences being statistical significant (p<0.05). These Doppler parameters. confirmed that, compared to the control group, the HFpEF group underwent abnormal decreases in e' and increases in E/e' and LAV Imax.

LA strain parameters

No statistically significant differences were detected between the two cohorts in LAEV, LAVmin, and LAVpreA (p>0.05). LAEF, LASr, LAScd, and LASct were all lower in the HFpEF group versus the control cohort (p<0.001), whereas LAVmax was higher, (p<0.05) (Table 4). These outcomes demonstrated that the LA strain parameters in HFpEF patients showed substantial differences compared with the healthy control subjects, and, importantly, these abnormalities could effectively indicate left ventricular dysfunction in patients.

ROC curve for LA parameters (Table 5, Figure 1)

Using LA strain parameters LASr, LAScd, and LASct as independent variables and HFpEF occurrence as the de-

Figure 1. Analysis of ROC curve results for LA strain parameters

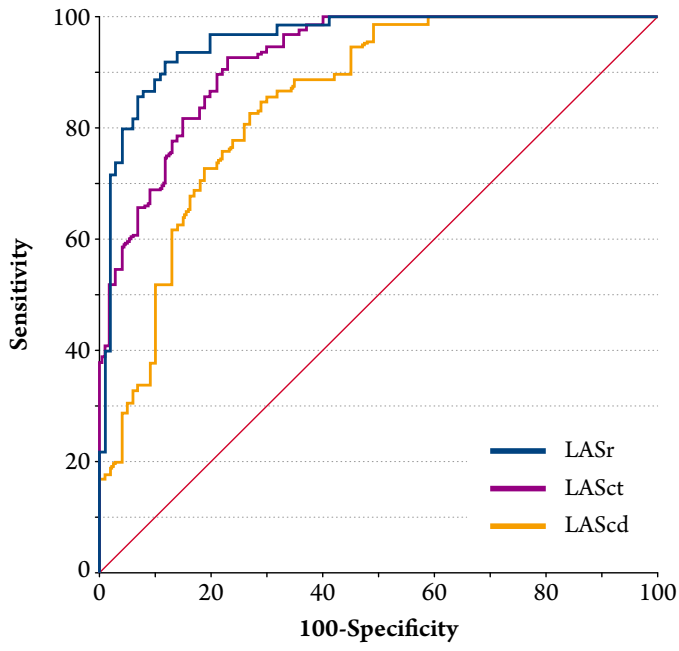

Table 6. Correlation analysis between LA strain parameters and NT-proBNP in HFpEF patients

Variables	NT-proBNP	
	r	p
LASr	–0.255	0.016
LAScd	–0.168	0.132
LASct	–0.203	0.079

LASr, LA strain during the reservoir phase; LAScd, LA strain during the conduit phase; LASct, LA strain during the contraction phase.

pendent variable, a ROC curve was plotted. The results showed that the diagnostic efficacy for HFpEF was optimal when LASr ≤34.65%, LAScd ≤17.85%, and LASct ≤17.02% (p<0.001 for each). The areas under the curve (AUC) were 0.959, 0.849, and 0.925, respectively.

*Correlation analysis between LA strain parameters and NT-proBNP in HFpEF (**Table 6**)*

A significant negative correlation existed between LASr and NT-proBNP (r=–0.255, p=0.016). No significant correlations were observed between LAScd and LASct with NT-proBNP (p=0.132 and p=0.079, respectively).

Discussion

This study conducted RT-3D-STI to assess LA function changes in patients with HHD HFpEF and their impact on the disease. The findings demonstrated that the HFpEF group had lower values of e', LAEF, LASr, LAScd, and LASct compared with the control cohort. In contrast, LAD, IVST, LVPWT, E/e', LAV Imax, and LAVmax were heightened in the HFpEF group. Additionally, a negative correlation was observed between LASr and NT-proBNP. Our outcomes align with those of previous studies. For instance, Meng et al. [14] noted that RT-3D-STI echocardiography could detect subtle myocardial dysfunction in patients with gout, despite normal ejection fractions.

HFpEF is particularly prevalent among individuals aged 65 yrs and older, and it represents the most frequent type of heart failure in this age group [15]. Patients often experience frequent hospitalizations due to symptoms such as shortness of breath, significant decline in physical strength, and edema, which severely impact their quality of life and lifespan [7, 16]. Despite the high incidence and mortality rates associated with HFpEF, which impose considerable stress on patients, families, and society at large, a clear pathophysiological mechanism has yet to be identified. Researchers generally believe that diastolic dysfunction of the LV may be central to the pathophysiological mechanism of HFpEF, which is often accompanied by left ventricular systolic dysfunction, LA dysfunction, and pulmonary hypertension [8, 17]. Nevertheless, the variability in clinical phenotypes and a limited understanding of the underlying pathophysiological mechanisms of HFpEF continue to obstruct identification of effective treatment strategies. Therefore, there is an immediate need for a straightforward and precise diagnostic method for HFpEF, so that its early treatment would improve patient prognosis and quality of life.

Echocardiography is a widely used, convenient, effective, and non-invasive method for evaluating and understanding cardiac structure and hemodynamics in patients with heart disease [18]. RT-3D-STI technology is a supplementary technique that enhances traditional echocardiography. It tracks the movement of ultrasound speckles in myocardial tissues based on the scattered myocardial images generated by the ultrasound beam. During the LV cardiac cycle, regions of interest are selected to generate motion patterns using software capable of measuring degrees of rotation and twist gradients. This method serves as a means for the visual assessment and measurement of the contraction and relaxation movements of the myocardium [19, 20]. However, RT-3D-STI has limitations due to the complex anatomical structure of the LA, such as being restricted to analyzing deformation in apical four-chamber and two-chamber views, making it difficult to track the true cross-plane motion of the myocardium.

RT-3D-STI, developed in recent years and based on full-volume scanning, offers a new ultrasound technique that synchronously displays three-dimensional images of myocardial motion and can comprehensively assess alterations in myocardial function in a short time [21–23]. Compared with two-dimensional speckle tracking technology, it can obtain three-dimensional motion images of the myocardium simultaneously, and its analysis software provides richer and more comprehensive data, enabling earlier and more accurate detection of myocardial abnormalities [24]. According to Nemes et al. [25], the overall longitudinal strain parameter of the LV derived from RT-3D-STI serves as a robust independent predictor of cardiovascular survival in healthy adults, and it also acts as an independent factor indicative of long-term event-free survival rates within this group. Additionally, research by Mutluer et al. [26] suggests that RT-3D-STI is a promising new approach for evaluating myocardial function, showing effective assessment of left ventricular strain and a strong correlation with LVEF.

Substantial changes were observed in overall longitudinal strain, radial strain, and circumferential strain parameters, indicating left ventricular remodeling and subclinical deformation. Similarly, Dogdus et al. [27] discovered that in patients with isolated coronary artery ectasia and embolization, overall longitudinal, radial, and circumferential strains were vigorously abated compared with healthy individuals, highlighting the substantial impact of this condition on left ventricular function. Both these studies and our research demonstrate that abnormalities in LA strain can be detected in HFpEF patients even when LA size appears normal, suggesting that LA

ISSN 0022-9040. Кардиология. 2025;65(8). DOI: 10.18087/cardio.2025.8.n2856

function may be subtly impaired prior to any visible remodeling. Several factors may contribute to this phenomenon:

1. LA myocardial fibrosis may be a key contributor to LA dysfunction;
2. Since the LA and LV are connected through the mitral valve annulus, any reduction in annular displacement speed or ventricular shifts could affect atrial motion.

Consequently, left ventricular systolic dysfunction may trigger LA dysfunction through atrioventricular coupling [28]. Furthermore, during mitral valve opening, the LA is exposed to left ventricular diastolic pressure during.

In the early stages of heart failure in HFpEF patients, LVEF may not yet change, but elevated end-diastolic pressure can increase LA pressure, resulting in increased mechanical stress and attenuated pulmonary venous drainage. As this process evolves and deteriorates, LA diastolic function and compliance become notably impaired, leading to decreased LA filling and ultimately culminating in LA enlargement and failure [29]. The ROC curve analysis demonstrated that when LASr ≤ 34.65%, LAScd ≤ 17.85%, and LASct ≤ 17.02%, the areas under the curves for diagnosing HFpEF was remarkedly high at 0.959, 0.849, and 0.925, respectively. Correlation analysis further showed a negative correlation between LASr and NT-proBNP, further reinforcing the significant importance of LA strain parameters for identifying early HHD HFpEF.

This study has several limitations. It is a retrospective clinical investigation conducted at a single center, and it involved a relatively small sample size. The diagnosis of patients was based solely on their signs and symptoms, NT-proBNP concentrations, and imaging outcomes. The diagnoses lacked support from invasive diagnostic procedures. Additionally, there is currently a lack of guidelines regarding atrial myocardial strain analysis software and normal strain value ranges for the atria. Moreover, the strain calculation methods used by data analysis systems from different manufacturers may vary, potentially leading to discrepancies between the resulting data and that reported here.

Conclusion

This study demonstrated that analysis of LA strain parameters can serve as a non-invasive method for quantitatively assessing LA dysfunction in patients with HFpEF. The importance of evaluating comprehensive echocardiographic parameters, particularly those related to LA function and diastolic mechanics, in HFpEF patients is discussed. These LA strain parameters may provide valuable insights into the underlying pathophysiological processes, and they may help guide treatment strategies aimed at improving outcomes in this challenging patient population.

Funding

Chongqing Science and Health Joint Medical Research Project 2022MSXM030

No conflict of interest is reported.

The article was received on 11/12/2024

REFERENCES

1. Hengel FE, Sommer C, Wenzel U. Arterial Hypertension. Deutsche Medizinische Wochenschrift. 2022;147(07):414–28. DOI: 10.1055/a-1577-8663
2. Slivnick J, Lampert BC. Hypertension and Heart Failure. Heart Failure Clinics. 2019;15(4):531–41. DOI: 10.1016/j.hfc.2019.06.007
3. Lau DH, Shenasa HA, Shenasa M. Hypertension, Prehypertension, Hypertensive Heart Disease, and Atrial Fibrillation. Cardiac Electrophysiology Clinics. 2021;13(1):37–45. DOI: 10.1016/j.ccep.2020.11.009
4. Nwabuo CC, Vasan RS. Pathophysiology of Hypertensive Heart Disease: Beyond Left Ventricular Hypertrophy. Current Hypertension Reports. 2020;22(2):11. DOI: 10.1007/s11906-020-1017-9
5. Díez J, Butler J. Growing Heart Failure Burden of Hypertensive Heart Disease: A Call to Action. Hypertension. 2023;80(1):13–21. DOI: 10.1161/HYPERTENSIONAHA.122.19373
6. Ballard-Hernandez J, Itchhaporia D. Heart Failure in Women Due to Hypertensive Heart Disease. Heart Failure Clinics. 2019;15(4):497–507. DOI: 10.1016/j.hfc.2019.06.002
7. Simmonds SJ, Cuijpers I, Heymans S, Jones EAV. Cellular and Molecular Differences between HFpEF and HFrEF: A Step Ahead in an Improved Pathological Understanding. Cells. 2020;9(1):242. DOI: 10.3390/cells9010242
8. Nair N. Epidemiology and pathogenesis of heart failure with preserved ejection fraction. Reviews in Cardiovascular Medicine. 2020;21(4):531–40. DOI: 10.31083/j.rcm.2020.04.154
9. Shams P, Malik A, Chhabra L. Heart Failure (Congestive Heart Failure). In: StatPearls -Treasure Island (FL): StatPearls Publishing; - 2025. [PMID: 28613623. Av. at: http://www.ncbi.nlm.nih.gov/books/NBK430873/]
10. Zawadzka M, Grabowski M, Kapłon-Cieślicka A. Phenotyping in heart failure with preserved ejection fraction: A key to find effective treatment. Advances in Clinical and Experimental Medicine. 2022;31(10):1163–72. DOI: 10.17219/acem/149728
11. Obokata M, Reddy YNV, Borlaug BA. Diastolic Dysfunction and Heart Failure With Preserved Ejection Fraction: Understanding Mechanisms by Using Noninvasive Methods. JACC: Cardiovascular Imaging. 2020;13(1 Pt 2):245–57. DOI: 10.1016/j.jcmg.2018.12.034
12. Jalali M, Behnam H. Speckle Tracking Accuracy Enhancement by Temporal Super-Resolution of Three-Dimensional Echocardiography Images. Journal of Medical Signals & Sensors. 2021;11(3):177–84. DOI: 10.4103/jmss.JMSS_26_20
13. Tadic M, Cuspidi C, Marwick TH. Phenotyping the hypertensive heart. European Heart Journal. 2022;43(38):3794–810. DOI: 10.1093/eurheartj/ehac393
14. Meng Y, Ma L, Zong T, Wang Z. Changes in the structure and function of the left ventricle in patients with gout: A study based on three-dimensional speckle tracking echocardiography. Journal of Clinical Ultrasound. 2023;51(7):1119–28. DOI: 10.1002/jcu.23501
15. Chen YJ, Liao PH, Hung CL. Diagnostic Yield and Model Prediction Using Wearable Patch Device in HFpEF. Studies in Health Technology and Informatics. 2024;315:25–30. DOI: 10.3233/SHTI240100
16. Shaik SP, Karan HH, Singh A, Attuluri SK, Khan AAN, Zahid F et al. HFpEF: New biomarkers and their diagnostic and prognostic

value. Current Problems in Cardiology. 2024;49(1):102155. DOI: 10.1016/j.cpcardiol.2023.102155
17. Silva MR, Sampaio F, Braga J, Ribeiro J, Fontes-Carvalho R. Left atrial strain evaluation to assess left ventricle diastolic dysfunction and heart failure with preserved ejection fraction: a guide to clinical practice: Left atrial strain and diastolic function. The International Journal of Cardiovascular Imaging. 2023;39(6):1083–96. DOI: 10.1007/s10554-023-02816-y
18. Berlot B, Bucciarelli-Ducci C, Palazzuoli A, Marino P. Myocardial phenotypes and dysfunction in HFpEF and HFrEF assessed by echocardiography and cardiac magnetic resonance. Heart Failure Reviews. 2020;25(1):75–84. DOI: 10.1007/s10741-019-09880-4
19. Zhu S, Lin Y, Zhang Y, Wang G, Qian M, Gao L et al. Prognostic relevance of left atrial function and stiffness in heart failure with preserved ejection fraction patients with and without diabetes mellitus. Frontiers in Cardiovascular Medicine. 2022;9:947639. DOI: 10.3389/fcvm.2022.947639
20. Sakaguchi E, Yamada A, Naruse H, Hattori H, Nishimura H, Kawai H et al. Long-term prognostic value of changes in left ventricular global longitudinal strain in patients with heart failure with preserved ejection fraction. Heart and Vessels. 2023;38(5):645–52. DOI: 10.1007/s00380-022-02211-y
21. Kadoglou NPE, Mouzarou A, Hadjigeorgiou N, Korakianitis I, Myrianthefs MM. Challenges in Echocardiography for the Diagnosis and Prognosis of Non-Ischemic Hypertensive Heart Disease. Journal of Clinical Medicine. 2024;13(9):2708. DOI: 10.3390/jcm13092708
22. Von Roeder M, Blazek S, Rommel K-P, Kresoja K-P, Gioia G, Mentzel L et al. Changes in left atrial function in patients undergoing cardioversion for atrial fibrillation: relevance of left atrial strain in heart failure. Clinical Research in Cardiology. 2022;111(9):1028–39. DOI: 10.1007/s00392-021-01982-0
23. Gao L, Lin Y, Ji M, Wu W, Li H, Qian M et al. Clinical Utility of Three-Dimensional Speckle-Tracking Echocardiography in Heart Failure. Journal of Clinical Medicine. 2022;11(21):6307. DOI: 10.3390/jcm11216307
24. Urbano-Moral JA, Arias-Godinez JA, Ahmad R, Malik R, Kiernan MS, DeNofrio D et al. Evaluation of myocardial mechanics with three-dimensional speckle tracking echocardiography in heart transplant recipients: comparison with two-dimensional speckle tracking and relationship with clinical variables. European Heart Journal – Cardiovascular Imaging. 2013;14(12):1167–73. DOI: 10.1093/ehjci/jet065
25. Nemes A, Kormányos Á, Olajos DL, Achim A, Ruzsa Z, Ambrus N et al. Long-Term Prognostic Impact of Three-Dimensional Speckle-Tracking Echocardiography-Derived Left Ventricular Global Longitudinal Strain in Healthy Adults – Insights from the MAGYAR-Healthy Study. Journal of Cardiovascular Development and Disease. 2024;11(8):237. DOI: 10.3390/jcdd11080237
26. Mutluer FO, Bowen DJ, Van Grootel RWJ, Roos-Hesselink JW, Van Den Bosch AE. Left ventricular strain values using 3D speckle-tracking echocardiography in healthy adults aged 20 to 72 years. The International Journal of Cardiovascular Imaging. 2021;37(4):1189–201. DOI: 10.1007/s10554-020-02100-3
27. Dogdus M, Kucukosmanoglu M, Kilic S. Assessment of the impact of isolated coronary artery ectasia on left ventricular functions with 3D speckle-tracking echocardiography. Echocardiography. 2019;36(12):2209–15. DOI: 10.1111/echo.14533
28. Kamel H, Elsayegh AT, Nazmi H, Attia HM. Assessment of left ventricular systolic function using two- and three-dimensional speckle tracking echocardiography among healthy preschool-age pediatric children. The Egyptian Heart Journal. 2022;74(1):21. DOI: 10.1186/s43044-022-00258-w
29. Nahar N, Haque T, Kabiruzzaman M, Khan MAM, Choudhury SR, Malik F. Assessment of subclinical left ventricular systolic dysfunction in patients with asymptomatic severe aortic stenosis with preserved left ventricular systolic function by three-dimensional speckle tracking echocardiography. Echocardiography. 2023;40(9):952–7. DOI: 10.1111/echo.15662

ISSN 0022-9040. Кардиология. 2025;65(8). DOI: 10.18087/cardio.2025.8.n2856